Video Article

Microfabrication of Nanoporous Gold Patterns for Cell-material Interaction Studies

Pallavi Daggumati[1], Ozge Kurtulus[2], Christopher Abbott Reece Chapman[3], Damla Dimlioglu[1], Erkin Seker[1]

[1]Department of Electrical and Computer Engineering, University of California, Davis

[2]Department of Chemical Engineering and Materials Science, University of California, Davis

[3]Department of Biomedical Engineering, University of California, Davis

Correspondence to: Erkin Seker at eseker@ucdavis.edu

URL: https://www.jove.com/video/50678
DOI: doi:10.3791/50678

Keywords: Bioengineering, Issue 77, Cellular Biology, Molecular Biology, Biomedical Engineering, Biochemistry, Chemistry, Chemical Engineering, Biophysics, Physics, Nanotechnology, Nanostructures, Biomedical Technology, Miniaturization, Gold, Staining and Labeling, Cell Culture Techniques, Microscopy, Electron Microscopy, Fluorescence, Nanotechnology, thin films (theory, deposition and growth), Nanoporous gold, cell culture, image analysis, microfabrication, nanotechnology, quantitative immunochemistry, scanning electron microscopy, SEM, fluorescence microscopy, stencil printing, photolithography, cell culture

Date Published: 7/15/2013

Citation: Daggumati, P., Kurtulus, O., Chapman, C.A., Dimlioglu, D., Seker, E. Microfabrication of Nanoporous Gold Patterns for Cell-material Interaction Studies. *J. Vis. Exp.* (77), e50678, doi:10.3791/50678 (2013).

Abstract

Nanostructured materials with feature sizes in tens of nanometers have enhanced the performance of several technologies, including fuel cells, biosensors, biomedical device coatings, and drug delivery tools. Nanoporous gold (np-Au), produced by a nano-scale self-assembly process, is a relatively new material that exhibits large effective surface area, high electrical conductivity, and catalytic activity. These properties have made np-Au an attractive material to scientific community. Most studies on np-Au employ macro-scale specimens and focus on fundamental science of the material and its catalytic and sensor applications. The macro-scale specimens limit np-Au's potential in miniaturized systems, including biomedical devices. In order to address these issues, we initially describe two different methods to micropattern np-Au thin films on rigid substrates. The first method employs manually-produced stencil masks for creating millimeter-scale np-Au patterns, while the second method uses lift-off photolithography to pattern sub-millimeter-scale patterns. As the np-Au thin films are obtained by sputter-deposition process, they are compatible with conventional microfabrication techniques, thereby amenable to facile integration into microsystems. These systems include electrically-addressable biosensor platforms that benefit from high effective surface area, electrical conductivity, and gold-thiol-based surface bioconjugation. We describe cell culture, immunostaining, and image processing techniques to quantify np-Au's interaction with mammalian cells, which is an important performance parameter for some biosensors. We expect that the techniques illustrated here will assist the integration of np-Au in platforms at various length-scales and in numerous applications, including biosensors, energy storage systems, and catalysts.

Video Link

The video component of this article can be found at https://www.jove.com/video/50678/

Introduction

Materials with nano-scale features have shown promise in enhancing various applications, including fuel cells[1], sensors[2,3], and biomedical devices[4,5]. A relatively new material is nanoporous gold (np-Au), which is produced by a nano-scale self-assembly process. The precursor to np-Au is a gold alloy that most commonly consists of silver at 60% to 80% by atomic percentage. Briefly, the characteristic open-pore nanostructure is the result of rearrangement of gold atoms in clusters as silver is dissolved by a strong acid (*e.g.* nitric acid 70%) or under an electrochemical potential[6-8]. Np-Au benefits from several desirable attributes, including large effective surface area, high electrical conductivity, well-established surface functionalization techniques, and biocompatibility[9]. Even though there has been a rapid expansion of studies on np-Au, most of them focus on np-Au's mechanical properties[10,11], catalytic activity[12], and biomolecular sensing performance[13-15]. While the desirable attributes are highly useful for several biomedical tools[16,17], the applications in this area have been limited. One possible reason for this is that most studies have predominantly used macro-scale specimens (*e.g.* sheets, foils, and ingots) and the techniques for incorporating np-Au in miniaturized systems have remained inadequate. In fact there are only a handful of examples of using conventional microfabrication techniques that employ np-Au films[16-20]. With the advent of miniaturization technology and the need for novel biomedical tools, it has become crucial to be able to integrate new materials into devices. This typically requires that the materials can be deposited and patterned with conventional microfabrication techniques. In addition, rapid quantification of cell-material interactions is commonly necessary to evaluate the biocompatibility of a new material. The goal of this paper is to demonstrate basic techniques to micropattern np-Au films and quantify both nanostructure and cell-material interactions via digital image processing.

Protocol

1. Nanoporous Gold Fabrication

1. Clean substrates in Piranha solution
    1. Add 25 ml hydrogen peroxide (30%) to 100 ml sulfuric acid (96%) in a crystallization dish and heat the mixture to 65 °C on a hotplate. CAUTION: The liquids are extremely corrosive and must be handled with care. The spent solution should not be stored in a sealed container, as it may explode.
    2. Place 1-inch by 3-inch microscope slides into the mixture using acid-resistant forceps and clean them for 10 min. Use a porcelain immunostaining boat for batch-cleaning small coverslips. Treat small coverslips with air plasma at 10 W for 30 sec prior to immersion into the solution.
    3. Rinse the cleaned samples in crystallization dishes under running deionized (DI) water for 3 min. Blow-dry samples with a nitrogen gun over lint-free towels.

2. Prepare stencil mask (Method 1: Use this for creating millimeter-scale patterns)
    1. Punch 250 µm-thick silicone elastomer sheets with biopsy punches and/or incise out regions with a scalpel over a semi-hard plastic surface. Clean the processed elastomer sheets in 70% isopropanol and dry with nitrogen gun.
    2. Place the punched sheet on a lint-free cleanroom towel and align the piranha-cleaned coverslips over the stencil with the sample surface facing the stencil.

3. Pattern lift-off photoresist (Method 2: Use this for creating sub-millimeter-scale patterns)
    1. Place a piranha-cleaned microscope slide on spinning chuck and blow off any particulates with nitrogen gun. Dispense 1.5 ml of adhesion promoter (hexamethyldisilazane) onto the glass slide using a plastic pipette. Spread the promoter by spinning the slide successively at 500 rpm for 5 sec and 1,500 rpm for 30 sec. Bake the slide on a hotplate at 115 °C for 7 min and let it cool for 5 min.
    2. Dispense 4 ml of photoresist onto the glass slide (3-inch by 1-inch). Spread the photoresist by spinning the slide with the same protocol as for the adhesion promoter. Bake the photoresist on a hotplate at 115 °C for 1.5 min and let it cool for 10 min.
    3. Expose the photoresist-coated slide with UV light (intensity: 22 mW/cm^2) through a transparency mask for 15 sec. Bake the photoresist on a hotplate at 115 °C for 1.5 min and wait for 45 min. Dissolve the exposed photoresist in the developer for at least 3.5 min. Rinse thoroughly with DI water. Inspect the developed patterns under an optical microscope.

4. Deposit precursor metals to produce np-Au thin films
    1. Load the samples into a sputtering machine that can independently deposit gold, silver, and chrome. Sputter-clean the samples for 90 sec at 50 W under 25 mTorr argon processing atmosphere before starting metal deposition.
    2. Sputter chrome for 10 min at 300 W under 10 mTorr argon. Sputter gold for 90 sec at 400 W under 10 mTorr argon. Co-sputter gold and silver for 10 min with silver at 200 W and Au power at 100 W. Turn off gold sputter source approximately 10 sec before turning off the silver sputter source.

5. Obtain precursor metal micropatterns
    1. Sonicate photoresist-coated samples in ~180 ml of photoresist stripper for 10 cycles of 20 sec sonication and 2 min pause between the cycles. Rinse the samples with DI water and dry with a nitrogen gun. Inspect the metal patterns under a microscope.
    2. Peel the elastomer stencil from non-photoresist coated samples using two tweezers to reveal the deposited metal.

6. Dealloy precursor metal and modify nanostructure via thermal treatment
    1. Fill a 200 ml glass beaker with 170 ml of nitric acid (70%) and maintain the solution temperature at 55 °C on a hotplate. CAUTION: The nitric acid is extremely corrosive and should be handled with appropriate protective equipment.
    2. Treat small coverslips with air plasma at 10 W for 30 sec prior to immersion into nitric acid. Place 1-inch by 3-inch microscope slides into the beaker using acid-resistant forceps and dealloy them for 15 min. Use a porcelain immunostaining boat for batch-dealloying small coverslips.
    3. Rinse the dealloyed samples by successively immersing them in two beakers filled with fresh DI water three times. Store samples in DI water and replace the water with fresh DI water every day for at least a week. Blow-dry samples with a nitrogen gun over lint-free towels before use.
    4. Load samples onto a clean silicon wafer in a rapid thermal processing equipment. Adjust the temperature to between 200 °C and 450 °C and the ramp rate to 10 °C/sec. Expose the samples to the prescribed temperature for 10 min under nitrogen ambient. Let the chamber cool (<100 °C) and remove the samples. Alternatively, slowly place the samples on the hotplate for thermal treatment.

2. Cell Culture

1. Prepare np-Au samples for cell culture
    1. Place np-Au samples in polystyrene dishes and treat with air plasma at 10 W for 30 sec and transfer the samples to 24-well tissue culture plates.
    2. Add 500 µl complete culture media (Dulbecco's Modified Eagle Medium with 10% fetal bovine serum and 1% penicillin/streptomycin) to each well. Store in a humidified incubator at 37 °C and 5% CO_2 until seeding the cells (<1 hr).

2. Maintain, passage, and seed cells
    1. Maintain cells of interest (in this case 3T3-NIH fibroblasts or murine astrocytes) in T75 flasks with culture media and passage when cells are 70% confluent.

2. For passaging the cells, remove media from the flask, wash twice with 10 ml phosphate buffered saline (PBS), add 2 ml of 1x Trypsin/EDTA and incubate until the cells detach (~5 min). Add 3 ml fresh media and centrifuge at 1,200 rpm for 3 min. Aspirate supernatant and suspend the pellet in 2 ml media.
3. Remove the spent media from the wells and seed the cells onto the glass coverslips at a density of 25,000 cells/cm^2 with a final volume of 1 ml. Shake the culture plate forward-back and right-left to ensure a uniform coating of cells over the samples. Incubate the cells until analysis while inspecting daily.

3. Cell and Material Analysis

1. Stain cells to visualize cytoskeleton and nuclei
    1. Remove spent media from wells and wash cells twice with PBS. Fix cells in 4% paraformaldehyde in PBS for 15 min.
    2. Prepare staining solution of 300 nM Alexa Fluor 488 phalloidin in PBS with 1% bovine serum albumin.
    3. Wash cells twice with PBS, and permeabilize them in 500 µl 0.1% Triton X-100 in PBS for 5 min.
    4. Wash cells twice with PBS and transfer them to clean wells. Blot 50 - 200 µl staining solution onto the samples and store in dark for 20 min.
    5. Wash cells with PBS and counter-stain with 3 nM of DAPI in PBS for 5 min.
    6. Wash cells with PBS, and dip in deionized water before mounting on glass cover slides with mounting media and seal with clear nail polish.

2. Acquire images of np-Au samples and cell cultures on np-Au surfaces
    1. Image np-Au surfaces with scanning electron microscope (SEM) with 50,000X magnification at 10 kV electron energy using secondary electron detector.
    2. Capture composite cell images at different spots on the samples using an inverted fluorescence microscope at 10X magnification with the appropriate filter cubes.

3. Process images to determine pore and cell morphology
    1. Open images in ImageJ and split into individual channels if applicable. Convert the images to 8-bit, subtract the background, and smooth them by median filtering. Adjust threshold either manually or by built-in thresholding algorithms to highlight the pores (voids) and cell bodies/nuclei.
    2. Use watershed command to separate merged pores or cells. Set particle analysis parameters and execute the command to extract number of particles, average area, and percent coverage by particles. Use DAPI-stained cell images for cell counting and phalloidin-stained cell images for quantifying percent cell coverage.
    3. Modify the included macro files to perform batch analysis of multiple images.

Representative Results

Figure 1 outlines the major procedural steps, including creating the np-Au patterns, culturing cells, quantifying the nanostructure, and characterizing cell morphologies. The elastomer stencil shown in **Figure 2a** (top) is used for creating the np-Au patterns shown in the images underneath. **Figure 2b** is a photograph of the porcelain boat for batch processing specimens. **Figure 2c** displays the color change of the deposited metal patterns before and after dealloying. The silvery finish (prior to dealloying) is due to the silver-rich alloy content. Upon dealloying, the film acquires a visibly orange-brown tint. **Figure 2d** illustrates the finer features produced by photolithographic patterning of the metal. Different pore morphologies can be obtained by thermal treatment of np-Au films[9], as shown in **Figure 3**. The cross-sectional image (**Figure 3**) reveals whether the films are dealloyed uniformly through the film thickness. The SEM images can be segmented (thresholded) into binary images (**Figure 3** bottom row) for determining the size and percent coverage by voids (**Code 1**). A representative fluorescence image of adherent murine astrocyte cells cultured on an np-Au surface is shown in **Figure 4**. The individual channels of the image can be split and segmented to produce binary images for analyzing cell-material interaction. Segmented cytoskeleton images can be used for quantifying cell area and surface coverage (**Code 2**), while the segmented cellular nucleus images are useful for cell counting (**Code 3**). **Figure 5** is a visual summary of common failures in fabrication of np-Au structures, including poor film adhesion, absence of porosity, and excessive thermal treatment.

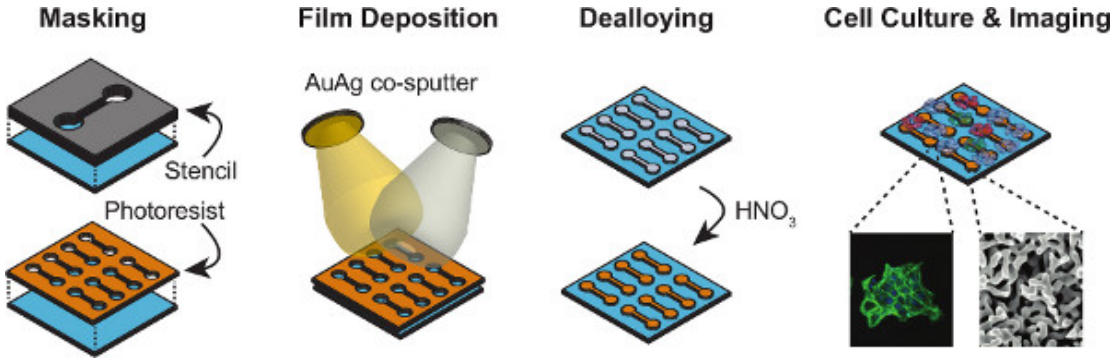

Figure 1. Schematic illustration of the major processing steps. Acid-cleaned substrates are either masked with a manually-cut stencil mask or photolithographically-patterned photoresist layer. The gold and silver targets are simultaneously sputtered to create a silver-rich gold alloy, where the masks transfer the patterns onto the glass substrates. Alloy patterns are dealloyed in nitric acid to create nanoporous gold (np-Au) patterns. Cells of interest are cultured on the samples and they are imaged with fluorescence and scanning electron microscopes to extract both biological and morphological features. Click here to view larger figure.

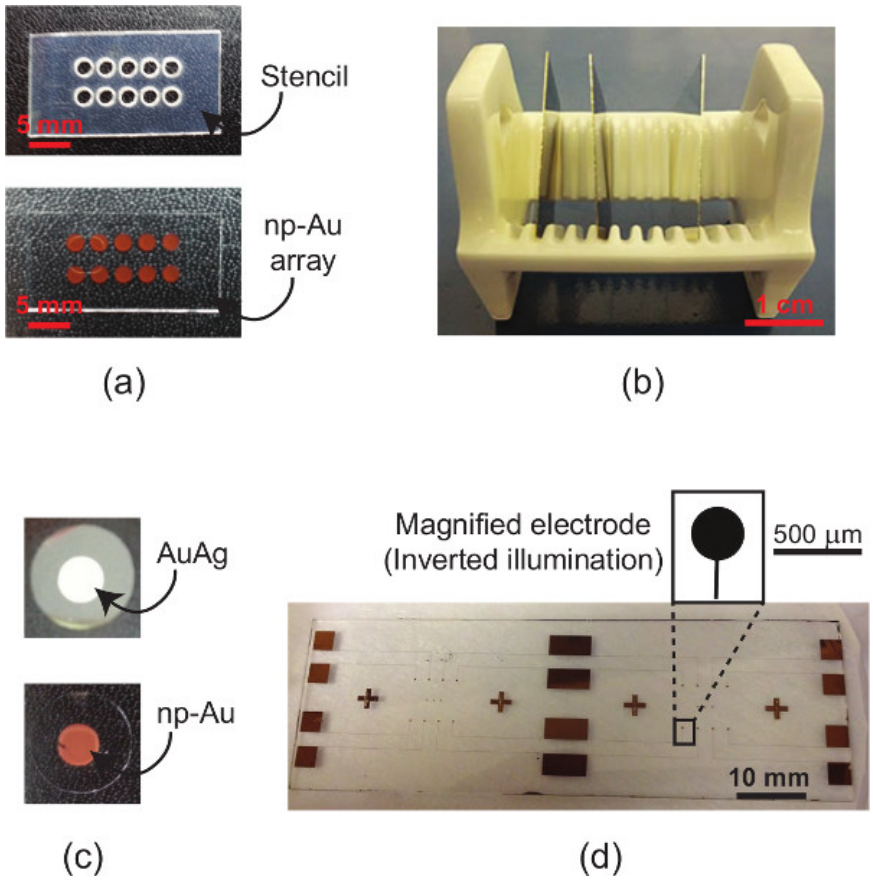

Figure 2. Optical images. (a) A silicone stencil (top) used for patterning precursor gold-silver alloy, which produces the np-Au array (bottom); **(b)** porcelain boat for batch processing specimens; **(c)** typical color of sputtered AuAg alloy (top) and dealloyed film (bottom); and **(d)** higher-resolution np-Au patterns produced by photolithographic masking during gold-silver deposition.

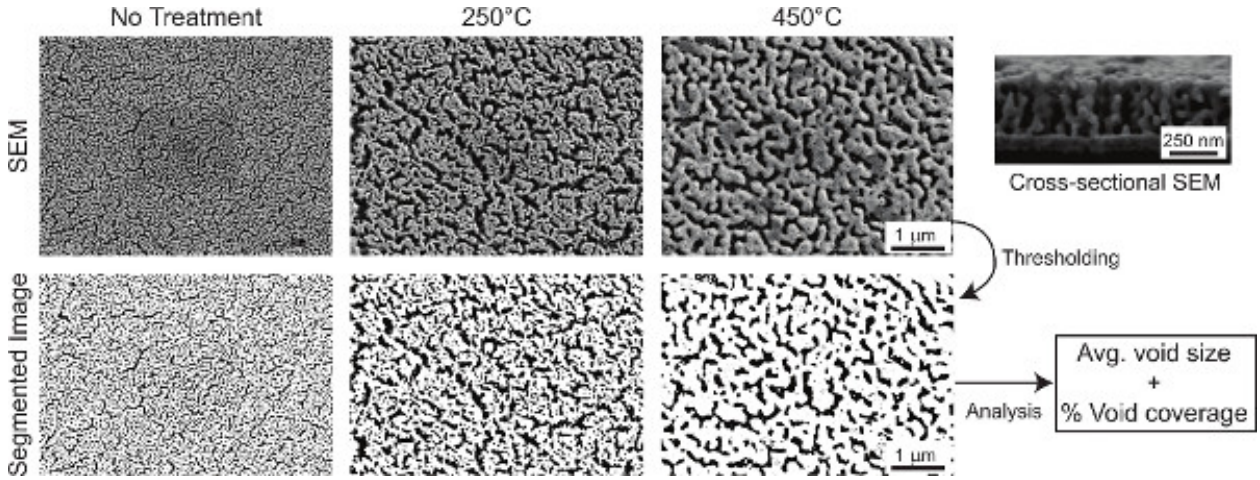

Figure 3. Np-Au SEM images (top row) and corresponding segmented images (bottom row) that are used for extracting average void size and percent void coverage. SEM image (top right) of a cleaved np-Au sample displays homogeneous pore structure through the film thickness. Click here to view larger figure.

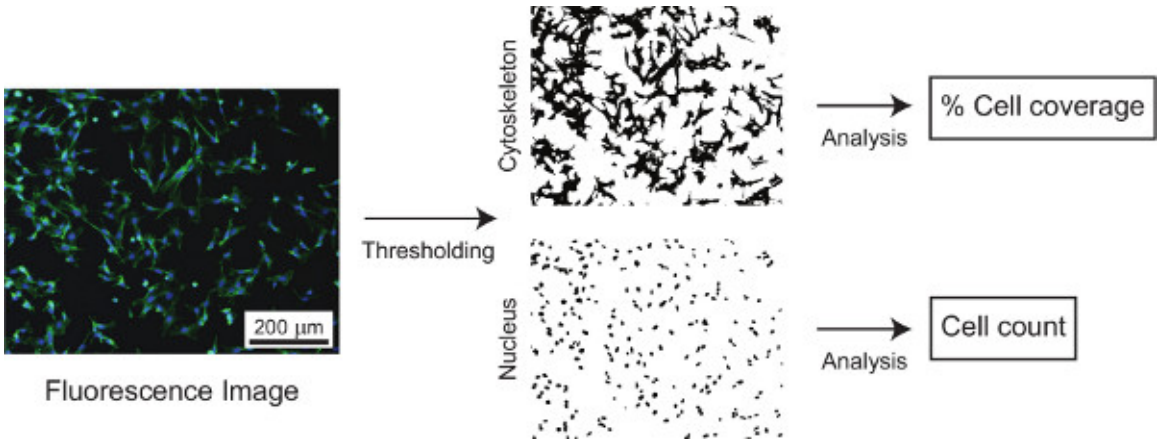

Figure 4. A composite f-actin (green) and nucleus (blue) stained cell image, which is segmented to extract percent cell coverage from the green channel and cell count from the blue.

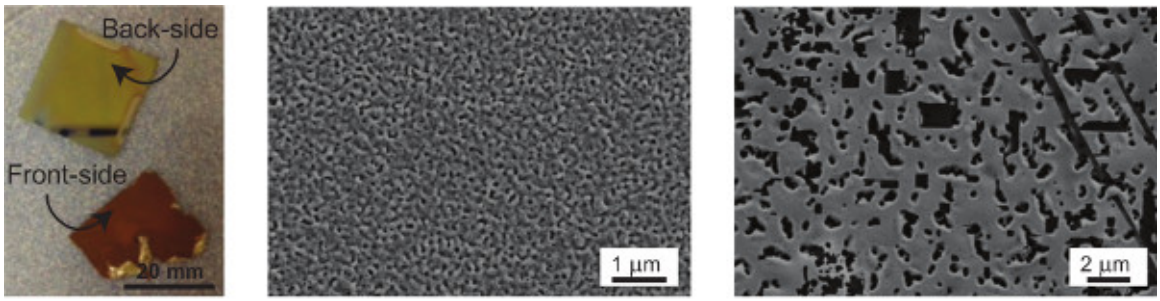

Figure 5. Images of typical failures. (a) delamination during dealloying due to an insufficient adhesive layer of chrome; **(b)** absence of porosity after dealloying due to insufficient silver content in the alloy; and **(c)** complete sintering of np-Au film due to thermal treatment temperature being too high.

Discussion

We demonstrate two different techniques to micropattern np-Au films for expanding use of these films in microsystems and biological studies. Sputter-coating gold and silver is a versatile method to create np-Au patterns, as sputtering is compatible with conventional microfabrication processes and the alloy composition and thickness can be easily controlled by varying the individual sputtering gun powers (for gold and silver targets) and the deposition time respectively. Typical np-Au film thicknesses range from 200 nm to 2 µm. The stencil method (Method 1, **Figure 2a**) using biopsy punches and scalpel allows for creating millimeter-scale patterns circumventing the need for photolithography. More complicated patterns can be produced by a programmable laser cutter. The compliant silicone elastomer stencil self-adheres onto glass surfaces, thereby preventing metal deposition underneath the mask and increasing pattern resolution. However, smaller features (<1 mm) are

typically difficult to produce with this method, as the thickness of the stencil prevents uniform metal deposition through the openings in the mask. Applications that require higher feature resolution can be attained with photolithographic patterning (Method 2, **Figure 2d**). The transparency masks to transfer patterns via photolithography can be obtained from several companies (*e.g.* Output City, Bandon, OR) and are economical alternatives to chrome-glass masks when minimum desired feature sizes are more than ~20 µm. The metal deposition onto the compliant stencil sometimes leads to detachment of the stencil from the substrate due to non-uniform stress generation. We typically mitigate this issue by securing the stencil to the underlying substrate by using a polyimide tape at the edges.

When smaller samples, such as circular coverslips (12 mm-diameter) typically used in our studies, porcelain boats shown in **Figure 2b** (commonly used for immunostaining applications) offer a convenient and economical means to process (*e.g.* clean, dealloy) multiple small samples. The batch processing of samples increases the uniformity of the produced nanostructure across different samples. Small samples tend to float when immersing into piranha or dealloying solutions, as they become hydrophobic when stored in air. Before any step requiring samples to be immersed in liquid, plasma treating them (10 W for 30 sec) renders the glass surface hydrophilic and helps to mitigate the floating issue. The most common problem in producing np-Au films is delamination during the dealloying step. This is typically attributed to tensile stress accumulation due to volume shrinkage during dealloying[21]. In order to prevent delamination, it is important to have strong adhesion between the np-Au film and the substrate. This is achieved by a sufficiently thick chrome (~150 nm) and intermediate gold layer (~200 nm). Deposited films should appear light to dark gray when viewed from the back side of a transparent substrate. The peeled film displayed in **Figure 5a** is a good example how the backside of the film should not look like - the gold finish indicates that the chrome layer is not sufficiently thick to ensure strong adhesion. Another reason for delamination is unclean sample surface, therefore it is essential to piranha-clean surfaces prior to metal deposition. In addition, it is important to make sure that the photoresist is fully-developed before depositing the film, as any residual photoresist prevents the strong adhesion of deposited metal onto the glass surface.

Thermal treatment of np-Au films is a convenient and controllable method for modifying pore morphology (**Figure 3**). While a rapid thermal annealing instrument is desirable for thermal treatment, furnaces and hotplates also produce acceptable results. The thermal dose and the temperature should be monitored carefully, as high temperatures (>500 °C) may lead to complete sintering of the np-Au and disappearance of porosity (**Figure 5c**). Insufficient silver content in the deposited alloy (less than 60% silver, at. %) also prevents porosity formation (**Figure 5b**).

In order to establish viable cell cultures on the aforementioned np-Au coated surfaces, it is important to soak the samples in DI water with several water changes to fully remove the nitric acid residue from the porous network. While it has not been necessary to treat the surfaces with specific extracellular matrix (ECM) proteins before seeding the cells, we observed that plasma treatment and soaking the samples in cell culture medium prior to seeding the cells drastically improve cell adhesion and viability. This improvement is most likely due to non-specific adsorption of adhesion proteins from the serum in cell culture media onto the np-Au surface. For cell culture conditions that require serum-free medium, it may be necessary to pre-treat the np-Au surface with ECM molecules (*e.g.* fibronectin).

For determining pore/void size and coverage, as well as cell count and cell coverage, images need to be converted to binary black & white images (see **Figures 3** and **4**) - the process is also known as *segmentation*. This requires picking a threshold gray value that is prone to user-bias. Therefore, absolute values determined by image processing should be reported with caution. Most studies require a comparison of different morphologies of cells and nanostructure; therefore, as long as the analysis parameters (*e.g.* threshold, particle size window) are kept consistent across samples, statistical significance can be attained with a relatively small number of samples. Prior to image segmentation, it is also helpful to smooth the images and subtract the background using the built-in commands in ImageJ (or a more specialized version, Fiji). We adjust the parameters in the included macro (**Supplemental Code Files 1-3**) to batch process multiple images.

We expect that the techniques demonstrated here will assist the scientific community in integrating np-Au into microsystems, including multiple electrode arrays for electrophysiology, biosensors, and miniature energy storage schemes. In addition, we believe that the semi-quantitative image processing methods will be valuable for a wide range of studies on the interaction of materials and adherent cells.

Disclosures

Authors have no conflicting financial interest.

Acknowledgements

O. Kurtulus and D. Dimlioglu are supported by a University of California Laboratory Fees Research Program Award 12-LR-237197. P. Daggumati is supported by a University of California Davis Research Investments in the Sciences & Engineering (RISE) Award. C.A. Chapman is supported by a Department of Education Graduate Assistance Areas of National Need Fellowship. This work was supported by UC Lab Fees Research Program, UC Davis RISE, and UC Davis College of Engineering start-up funds.

References

1. Arico, A.S., Bruce, P., Scrosati, B., Tarascon, J.M., & Van Schalkwijk, W. Nanostructured materials for advanced energy conversion and storage devices. *Nature Materials.* **4**, 366-377 (2005).
2. Roy, S. & Gao, Z. Nanostructure-based electrical biosensors. *Nano Today.* **4**, 318-334 (2009).
3. Chen, C.L., *et al.* DNA-decorated carbon-nanotube-based chemical sensors on complementary metal oxide semiconductor circuitry. *Nanotechnology.* **21**, 095504 (2010).
4. Lu, J., Rao, M.P., MacDonald, N.C., Khang, D., & Webster, T.J. Improved endothelial cell adhesion and proliferation on patterned titanium surfaces with rationally designed, micrometer to nanometer features. *Acta Biomaterialia.* **4**, 192-201 (2008).
5. Wagner, V., Dullaart, A., Bock, A.K., & Zweck, A. The emerging nanomedicine landscape. *Nat. Biotechnol.* **24**, 1211-1218 (2006).
6. Weissmüller, J., Newman, R., Jin, H., Hodge, A., & Kysar, J. Theme Article - Nanoporous Metals by Alloy Corrosion: Formation and Mechanical Properties. *Materials Research Society Bulletin.* **34**, 577-586 (2009).

7. Erlebacher, J., Aziz, M., Karma, A., Dimitrov, N., & Sieradzki, K. Evolution of nanoporosity in dealloying. *Nature.* **410**, 450-453 (2001).
8. Okman, O., Lee, D., & Kysar, J.W. Fabrication of crack-free nanoporous gold blanket thin films by potentiostatic dealloying. *Scripta Mater.* **63**, 1005-1008 (2010).
9. Seker, E., Reed, M., & Begley, M. Nanoporous Gold: Fabrication, Characterization, and Applications. *Materials.* **2**, 2188-2215 (2009).
10. Biener, J., *et al.* Size effects on the mechanical behavior of nanoporous Au. *Nano Lett.* **6**, 2379-2382 (2006).
11. Senior, N. & Newman, R. Synthesis of tough nanoporous metals by controlled electrolytic dealloying. *Nanotechnology.* **17**, 2311-2316 (2006).
12. Zielasek, V., *et al.* Gold catalysts: Nanoporous gold foams. *Angew. Chem. Int. Ed.* **45**, 8241-8244 (2006).
13. Wittstock, A., Biener, J., & Bäumer, M. Nanoporous gold: a new material for catalytic and sensor applications. *PCCP.* **12**, 12919-12930 (2010).
14. Shulga, O., *et al.* Preparation and characterization of porous gold and its application as a platform for immobilization of acetylcholine esterase. *Chem. Mater.* **19**, 3902 (2007).
15. Shulga, O., Zhou, D., Demchenko, A., & Stine, K. Detection of free prostate specific antigen (fPSA) on a nanoporous gold platform. *The Analyst.* **133**, 319-322 (2008).
16. Seker, E., *et al.* The fabrication of low-impedance nanoporous gold multiple-electrode arrays for neural electrophysiology studies. *Nanotechnology.* **21**, 125504 (2010).
17. Seker, E., Berdichevsky, Y., Staley, K.J., & Yarmush, M.L. Microfabrication-Compatible Nanoporous Gold Foams as Biomaterials for Drug Delivery. *Advanced Healthcare Materials.* **1**, 172-176 (2012).
18. Okman, O. & Kysar, J.W. Microfabrication of Nanoporous Gold. *Nanoporous Gold: From an Ancient Technology to a High-Tech Material.* **22**, 69 (2012).
19. Lee, D., *et al.* Microfabrication and mechanical properties of nanoporous gold at the nanoscale. *Scripta Mater.* **56**, 437-440 (2007).
20. Seker, E., *et al.* The effects of post-fabrication annealing on the mechanical properties of freestanding nanoporous gold structures. *Acta Mater.* **55**, 4593-4602 (2007).
21. Parida, S., *et al.* Volume change during the formation of nanoporous gold by dealloying. *Phys. Rev. Lett.* **97**, 35504-35506 (2006).

